HHS Public Access

Author manuscript

Acta Biomater. Author manuscript; available in PMC 2024 October 15.

Published in final edited form as:

Acta Biomater. 2023 October 15; 170: 97–110. doi:10.1016/j.actbio.2023.08.036.

Pentagalloyl Glucose-stabilized Decellularized Bovine Jugular Vein Valved Conduits as Pulmonary Conduit Replacement

Dipasha Sinha[1], **Agnes Nagy-Mehesz**[1], **Dan Simionescu**[1], **John E. Mayer Jr**[2], **Naren Vyavahare**[1]

[1]Department of Bioengineering, College of Engineering, Computing and Applied Sciences, Clemson University, Clemson, South Carolina, 29634, USA.

[2]Department of Cardiac Surgery, Boston Children's Hospital, Boston, Massachusetts; Department of Surgery, Harvard Medical School, Boston, Massachusetts, 02115, USA.

Abstract

Congenital heart diseases (CHD) are one of the most frequently diagnosed congenital disorders, affecting approximately 40,000 live births annually in the United States. Out of the new patients diagnosed with CHD yearly, an estimated 2,500 patients require a substitute, non-native conduit artery to replace structures congenitally absent or hypoplastic. Devices used for conduit replacement encounter limitations exhibiting varying degrees of stiffness, calcification, susceptibility to infection, thrombosis, and a lack of implant growth capacity. Here, we report the functionality of pentagalloyl glucose (PGG) stabilized decellularized valved bovine jugular vein conduit (PGG-DBJVC). The PGG-DBJVC tissues demonstrated mechanical properties comparable to native tissues while exhibiting more resistance to enzymatic degradation. Subcutaneous implantation of tissues established their biocompatibility and resistance to calcification, while implantation in sheep in the pulmonary position demonstrated adequate implant functionality, and repopulation of host cells, without excessive inflammation.

In conclusion, this PGG-DBJVC device could be a favorable replacement option for pediatric patients, reducing the need for reoperations required with current devices.

Graphical Abstract

Conflict of Interest:
The Principal Investigator, Narendra Vyavahare, is a significant shareholder in Annoviant Technologies, LLC, which has licensed this technology; however, the research work was performed independently.

Declaration of Interest:
Narendra Vyavahare is a significant shareholder in Annoviant Inc., which has licensed PGG stabilization technology; however, the research work was performed independently with NIH STTR funding.

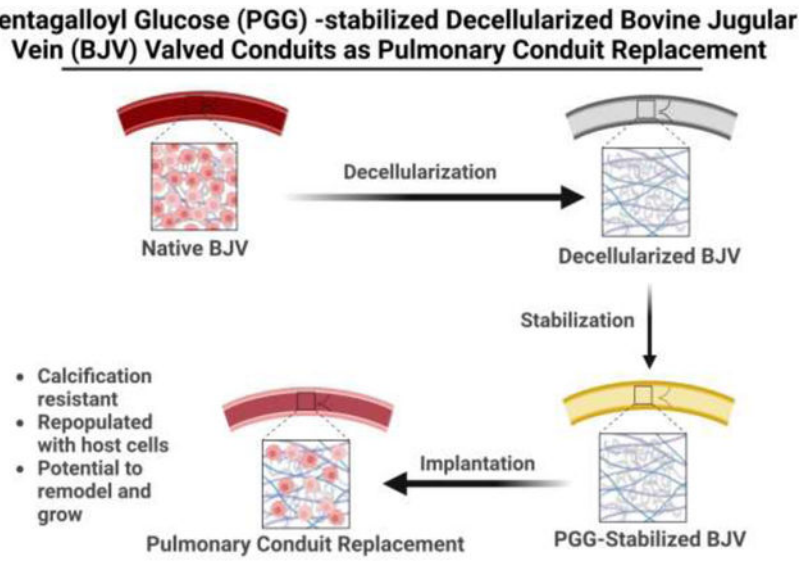

Keywords

Congenital Heart Diseases (CHD); Tissue Engineering; Bovine Jugular Vein (BJV); Decellularized Scaffolds; Right Ventricular Outflow Tract (RVOT) Replacement

1. Introduction:

Pediatric CHD patients often require pulmonary conduit replacements to correct critical congenital conditions like pulmonary stenosis, tetralogy of Fallot, pulmonary atresia, truncus arteriosus, and transposition of the great arteries along with ventricular septal defects [1–4]. Currently used homografts, glutaraldehyde crosslinked xenografts (Contegra), or synthetic grafts are suboptimal. Calcification, thrombosis, and the inability to remodel require multiple replacement surgeries [5–8]. Data reviewed from ~300 pediatric patients who underwent placement of the right ventricle-to-pulmonary artery valved conduit using glutaraldehyde-treated tissues concluded that stenosis leading to the xenograft conduit failure was present in all types of implants [9]. A CDRH (Center for Devices and Radiological Health, FDA) report for Contegra grafts showed 44% stenosis, 42% device replacement, and a subsequent valved conduit or valve replacement required in 79 out of 84 pediatric patients undergoing implantation [10]. One of the main reasons for calcification, stenosis, and immune response in glutaraldehyde-fixed xenografts may be related to the remnant bovine cellular material, such as membrane phospholipids since these conduits are not decellularized before glutaraldehyde treatment. Efforts have been made to develop pulmonary valve conduits from decellularized xenograft tissues, but results are mixed. The initial iteration of the SynerGraft® valve (CryoLife, Inc., Kennesaw, GA, USA.), a porcine xenograft, showed promising preliminary results in adults but elicited a severe immune response and catastrophic failures in children, primarily due to incomplete decellularization [11]. Pulmonary conduits were also developed with decellularized porcine small intestinal submucosa. A recent publication showed that such valved conduits failed due to thrombosis and calcification and demonstrated little, if any, remodeling when implanted in sheep

[12]. Matrix P® decellularized porcine tissue scaffolds were tried as pulmonary conduits; however, they showed unfavorable results with a high rate of reoperation/reintervention for structural pulmonary valve failure and aneurysms [13]. Another approach that has shown promise utilizes polymer-based scaffolds that allow host cell repopulation, developed by XELTIS, a European-based company that initiated a ten-patient clinical trial for pulmonary valve conduit in children in 2019 [14, 15].

With the limited success of these different strategies, there is still a need to develop an optimal replacement conduit for pediatric patients that can last for several decades. Such a conduit should provide optimum mechanical strength on implantation, allow cellular infiltration, and be able to remodel over time, thereby displaying a potential to grow along with the patient [16]. To develop such a conduit, we used decellularized bovine jugular vein that was stabilized with pentagalloyl glucose (PGG) (PGG-DBJVC). Bovine jugular veins have a tri-leaflet valvular apparatus, making it an attractive option as a pulmonary conduit replacement. Decellularization removes the scaffold's immunogenic cellular components while preserving the extracellular matrix structure.

Decellularization might lead to the loss of ECM integrity, increased degenerative structural failure, and calcification after implantation [17, 18]. To optimize the biodegradation process and maintain ECM integrity, crosslinking or stabilization of decellularized ECM is utilized. PGG is a non-cytotoxic polyphenolic tannin composed of a hydrophobic inner core and numerous external hydroxyl groups, which specifically binds to hydrophobic regions of proteins and form several hydrogen bonds [19, 20]. NMR studies have shown that PGG has a strong affinity for proline-rich proteins like elastin and collagen, binding through the hydrophobic stacking of the polyphenol ring against the pro-S surface of proline [21, 22]. The addition of PGG *in vitro* has been shown to increase the rate of coacervation and self-assembly of tropoelastin, a precursor to elastin fibers within the ECM [23]. While glutaraldehyde fixation crosslinks only the collagen fibers, PGG binds to both collagen and elastin [24]. Since ~50% of the dry weight of vascular tissues is composed of elastin [25], stabilization of elastin is essential in maintaining the structure and mechanical behavior of native vascular tissues.

Furthermore, PGG is one of the most potent antioxidant within the tannin group and is also known for its antimicrobial, antiviral, anti-diabetic, anti-inflammatory, and anti-tumor properties[26–28]. PGG-treated elastin-rich tubular vascular grafts (ETVGs) have shown good mechanical and biological properties in multiple *in vivo* subdermal implantation models, reducing rapid biodegradation and calcification of the implants [29, 30]. This study aimed to create a replacement conduit that is easy to suture, compliant, resistant to thrombosis, aneurysmal degradation, and calcification, and allows host cell repopulation and remodeling.

2. Materials and Methods:

2.1 Fabrication of decellularized bovine jugular vein scaffolds:

Fresh bovine jugular vein tissues, collected from UDSA-certified slaughterhouses, were obtained from Animal Technologies, Inc (Tyler, TX). After the removal of blood and

trimming of fats and adventitious tissue, the native tissues were incubated with 0.05 M sodium hydroxide (NaOH) for one hour at room temperature, followed by treatment with a decellularizing solution composed of 0.25% sodium dodecyl sulfate (SDS) (Fisher BP349–100), 0.5% sodium Deoxycholate (DOC) (Carolina Biological 858740), 0.5% Triton X 100 (Alfa Aesar A16046), and 0.2% Ethylene Diamine Tetra-Acetic acid (EDTA) (Sigma Aldrich E6511) in 50 mM TRIS (tris (hydroxymethyl) amino-methane) (Bio-Rad 1610716) buffer (pH 7.4 ± 0.05) for six days. The decellularization solution was replaced every two days. To remove traces of detergents and remnant nuclear material, decellularized tissues were washed with 70% ethanol, followed by incubation with 360 U/mL DNase (Worthington, LS002139) and 360 U/mL RNase (Fisher, BP25392501) solutions for four days at 37°C, with solution replacement every 24 hours [31]. Sterilization of scaffolds was performed with filter sterilized 0.1% Peracetic acid (pH 7.4 ± 0.05) at room temperature for 2 hours, and the final sterile, decellularized scaffolds (DBJVC) were either lyophilized, processed for histology, or treated with PGG as described below.

2.2 DNA Quantification:

Native and DBJVC tissues (5–10 mg) (wall and leaflet portions of BJV) were lyophilized, and their initial dry weight was recorded. DNA extraction was performed using Qiagen Dneasy Blood and Tissue Kit (Cat. No. 69504) as per the manufacturer's instructions. The extracted DNA was quantified with the Quant-It Pico Green dsDNA Reagent kit (Fisher, P11496), according to the manufacturer's instructions. Concentration was calculated from the standard curve, and the total amount of DNA was normalized to the initial dry weight of the tissue and expressed as ng DNA/ mg dry weight.

2.3 Treatment with Pentagalloyl Glucose (PGG):

PGG solutions were prepared in 20% Isopropanol in 50 mM 2-[4-(2-hydroxyethyl) piperazin-1-yl] ethane sulfonic acid (HEPES) buffer at pH 5.5. Decellularized valved Bovine Jugular Vein (DBJV) conduits were treated with PGG concentrations ranging from 0.05% to 3.33% to determine the concentration at which tissue stabilization was maximal. PGG treatment was conducted for 20 ± 2 hours at room temperature, protected from light, followed by extensive washing with PBS (6 cycles of 30 minutes) to remove any excess PGG. Subsequently, PGG-treated tissues were lyophilized, processed for histology, or stored in sterile PBS with 1% Penicillin Streptomycin at 4°C for up to 24 months for long-term storage analysis.

2.4 Glutaraldehyde fixation of native tissues:

Native BJV tissues, after removal of blood and adventitia, were treated with 0.6% glutaraldehyde in 50 mM HEPES buffered saline (pH 7.4) at room temperature. After 24 hours, the solution was replaced with 0.2% glutaraldehyde in 50 mM HEPES (pH 7.4), and crosslinking was allowed for up to 6 days [32]. Glutaraldehyde-fixed native tissues were subsequently used as controls for comparison of PGG-DBJVC tissues.

2.5 PGG extraction and quantification:

PGG-DBJVC samples were lyophilized, and their initial dry weights were recorded. Extraction of PGG from the lyophilized tissues (15–20 mg) was conducted in 1 ml of 80% methanol at room temperature by shaking for a total of 30 minutes. The methanol extract was quantified using Folin-Ciocalteu (F-C) Regent (Sigma-Aldrich, 47641) based on a method adapted from literature as described previously [33–35]. Briefly, 800 μl of F-C reagent, diluted 1:10 with DI water, was added to 200 μl of extract, vortexed, and incubated at 37°C for 5 minutes; following which, 600 μl of 7.5% sodium carbonate (Alfa Aesar, L13098.36) was added, vortexed, and incubated at 37°C for 30 minutes. At the end of the assay, absorption was read at 760 nm. The PGG concentration of the methanolic extract was calculated from the plotted PGG standard curve. The total amount of PGG extracted for each tissue sample was normalized to the initial weight of the sample.

2.6 Resistance to Elastase and Collagenase enzyme activity:

Approximately 15–30 mg of lyophilized native, glutaraldehyde fixed native, DBJVC, or PGG-DBJVC tissues were weighed and subjected to treatment with elastase and collagenase to determine the ability of scaffolds to resist rapid degradation by these enzymes. For the elastase challenge, tissues were placed in 1.2 mL of 10 U/mL Elastase (EPC Elastin Products, EC134) with 1 mM Calcium Chloride (Sigma, C7902), 0.02% Sodium Azide (Sigma, S2002) in 100 mM TRIS (Bio-Rad, 161–0716) buffer (pH 7.8 ± 0.05) for 24 hours. For the collagenase treatment, 1.2 mL of 75 U/mL Collagenase type 1 (Worthington, LS004194) was used with 10 mM Calcium Chloride and 0.02% Sodium Azide in 50 mM TRIS buffer (pH 8 ± 0.05) for 48 hours. Both assays were conducted at 37°C under continuous shaking. At the end of the respective time periods, the enzyme solution was removed, the remaining tissues were lyophilized, and their final weights were recorded. The weight loss was calculated and expressed as a percentage of the initial weight loss (%).

2.7 Long-Term Storage Analysis:

PGG-DBJVC samples were stored in sterile PBS with 1% Penicillin Streptomycin at 4°C, 30–50% humidity conditions, for up to 24 months for long-term storage analysis. Samples retrieved after intervals of 6 months, 9 months, 13 months, 16 months, and 24 months from initial preparation were lyophilized and subjected to PGG extraction and Collagenase and Elastase enzyme assays as described earlier. The PGG content of the tissues after storage and their resistance to enzyme degradation was compared to freshly prepared PGG-DBJVC (0 months storage) to determine the stability of the PGG-crosslinking of the tissues.

2.8 Histological Analysis:

Tissue samples were fixed in 10% neutral buffered formalin for 24 hours at room temperature, embedded in paraffin, and sectioned at 5 μm thickness. The sections were deparaffinized, rehydrated, and stained separately with DAPI (4’, 6- diamidino- 2-phenylindole) and Hematoxylin-Eosin (H&E) to determine the cellular component of the tissues and various stains such as Masson Trichrome for collagen, Verhoeff Van Gieson (VVG) for elastin fibers, and Alizarin Red for calcium deposits were used. Images were

captured with an Axiovert 40 CFL (Zeiss) inverted microscope with a MicroFire (Optronics) digital camera.

2.9 Suture retention testing:

The suture retention test was performed based on a method adapted from ISO 7198: 2016 Cardiovascular implants-Tubular vascular prostheses [36–38]. Rectangular strips of 3 cm x 1 cm were excised from native, decellularized, PGG-DBJVC, and glutaraldehyde-fixed native BJV conduit walls in both circumferential and longitudinal directions. The bottom 1 cm of each strip was secured in the lower clamp of a uniaxial tester, Instron 5944, equipped with 50 N load cell (Norwood, Massachusetts, USA). A 4–0 coated Vicryl suture (Ethicon) was inserted through the tissue at 0.2 cm from the opposite end of the strip and secured into the upper clamp of the uniaxial tester. Samples were pre-loaded to 0.01 N and stretched at a rate of 1 mm/sec until tissue failure. Samples thickness (averaged from 3 different locations), maximum displacement, and the maximum force at failure were recorded. The stretch ratio, defined as maximum displacement/ initial length, as well as compliance, defined as maximum force at failure/ stretch ratio, of the tissue was calculated.

2.10 Biaxial tensile testing:

For the mechanical characterization of bovine jugular vein conduits, a biaxial tensile testing procedure was used as described in literature [39]. Tissue samples (1 cm x 1 cm) were excised from native, decellularized, PGG-DBJVC, and glutaraldehyde-fixed native BJV conduit walls. A biaxial tester, the BioTester 5000 (CellScale, Waterloo, Canada), equipped with a load cell of 23 N load capacity, was used to perform the testing. Each edge of the sample was gripped using a Cell Scale Bio Rake system to mount the samples, with five rigid tungsten “tines,” restricting sample shear deformation [40]. Samples were preloaded to 10 mN and stretched to 100% displacement at a rate of 5% displacement/second. During the testing, displacement, and force data were collected and based on the sample dimensions and output data, corresponding nominal stress (i.e., engineering stress), true strain values were calculated, and stress-strain curves were plotted within the ranges of 0% - 100% strain. Young’s modulus for the samples were calculated at the physiologically relevant region of the stress-strain curves between 10% and 20% strain.

2.11 Cytotoxicity in *in vitro* cell cultures:

The potential biological reactivity of L929 mouse fibroblast cells in response to exposure to PGG-DBJVC extract was examined. The cytotoxicity study was conducted at Toxikon, Bedford, MA, in compliance with FDA 21 CFR, part 58 GLP conditions for Nonclinical Laboratory Studies. The cytotoxicity results of the extracts were analyzed according to ISO 10993–5 guidelines.

2.12 Intracutaneous Injection:

PGG-DBJVC extracts were evaluated for their potential to produce irritation after intracutaneous injection in New Zealand White rabbits (n=3). This study was conducted at Toxikon, Bedford, MA, in compliance with FDA 21 CFR, part 58 GLP conditions

for Nonclinical Laboratory Studies, and based upon ISO 10993–10, ISO 10993–12, and ISO/IEC 17025.

2.13 Sensitization:

Extracts of PGG-DBJVC were analyzed for potential allergenic or sensitization capacity by the Kligman Maximization test in Hartley guinea pigs (n=35). This study was conducted at Toxikon, Bedford, MA, in compliance with FDA 21 CFR, part 58 GLP conditions for Nonclinical Laboratory Studies. The evaluation of skin reactions used the four-point scale described in Figure S2. Any animal showing a skin reaction score of 1 or greater (at any time point) was considered positive. Based on ISO 10993–10 guidelines, a sensitizer was defined as an article with a positive response observed in at least 10% of the test animals.

2.14 Subcutaneous Implantation in rats:

PGG-DBJVC and glutaraldehyde fixed native BJV leaflets and walls were implanted subcutaneously in 3–4-week-old Sprague Dawley (SD) rats to assess the biocompatibility of the scaffolds. Forty-two rats were used, 21 were implanted with the conduit wall, and 21 had leaflet samples implanted.

Each rat received a glutaraldehyde-fixed (leaflet/wall) and a PGG-treated (leaflet/wall) sample at separate sites. For the surgical procedure, the rats were anesthetized by inhalation of isoflurane. A 1 cm incision was made, and subcutaneous pockets were created below each shoulder of the rats under an aseptic technique. Pre-prepared sterile implants (PGG-treated decellularized or glutaraldehyde-fixed native leaflets or walls) were placed into separate pockets, and the wounds were closed with surgical staples. The animals were allowed to recover and housed in animal quarters for 1 and 3 months follow-up periods. At the designated time intervals (30- or 90-days post-implant), rats were euthanized, and implants were retrieved. All retrieved implants were examined macroscopically and processed for histological examination or ICP (Inductively Coupled Plasma) elemental analysis. Major organs (spleen, liver, kidney) were also collected and processed for histological analysis to evaluate general cytotoxicity. All surgeries and animal handling were done under an Institutional Animal Care and Use Committee (IACUC) approved animal use protocol.

2.15 Inductively Coupled Plasma (ICP) Spectroscopy Calcium and Phosphorous mineral analysis:

Upon retrieval, the subcutaneous implant samples were frozen, lyophilized, weighed, and acid hydrolyzed in 2 mL of 6 N hydrochloric acid (HCl) overnight at 37°C. Acid hydrolyzed samples were dried under nitrogen gas at 96°C, and the residue was resuspended in 0.1 N HCl. Resuspended samples were filtered to remove any solid particles. Calcium and phosphorous content within these samples were analyzed using the Spectro Acros I.C.P. Spectrometer (SPECTRO Analytical Instruments, Kiev, Germany) [41]. Elemental concentrations were normalized to the initial dry sample weights.

2.16 Immunofluorescence (IF) analysis:

Histological tissue sections were deparaffinized, rehydrated, followed by heat-mediated antigen retrieval with corresponding buffers (citrate or TRIS/EDTA). Sections were

permeabilized with 0.1% Triton and incubated for 1 hour with Background Buster for specific and non-specific blocking (Innovex Biosciences NB306). Glutaraldehyde fixed samples were treated with 0.01M Glycine for aldehyde blocking before primary antibody incubation. Incubation with the primary antibodies was performed overnight at 4°C. Infiltration of fibroblast/myofibroblast cells were characterized using mouse anti-α-Smooth Muscle Actin (αSMA) (1:200, Novus Biologicals NBP2–33006), mouse anti-Vimentin (1:100, Novus Biologicals NBP2–44832) and mouse anti-HSP47 (1:100, Enzo Life Science ADI-SPA 470). Immune cell infiltration was characterized using mouse anti-CD68 (1:100, Abcam ab630), mouse anti-CD163 (1:100, Bio-Rad M.C.A. 342GA), mouse anti-CD80 (1:100, B.D. Biosciences 555012), mouse anti-CD3 (1:100, B.D. Biosciences 556970), and mouse anti-CD11c (1:100, Bio-Rad) primary antibodies. Cy3 conjugated donkey anti-mouse (Jackson Laboratories, 715–165-150) secondary antibody incubation was done for 1 hour at room temperature, protected from light. After intensive washing, sections were counterstained with DAPI nuclear staining, cover-slipped with water-based mounting solution (FluoroGel), imaged using Keyence BZ-X810 all in one microscope, and analyzed using ImageJ Fiji software [42]. All images were captured at the same intensity and exposure settings. The expression of the specific antigens was semi-quantified using a protocol adapted from the literature [43]. The DAPI and Cy3 images were analyzed separately after threshold adjustment to determine the mean grey value of positive staining. The mean grey value calculated from the Cy3 image was divided by the nuclear area obtained from the DAPI image to quantify the positive IHC staining semi-quantitatively. The staining procedure without the primary antibody served as a negative control.

2.17 Implantation of PGG-treated Bovine Jugular Vein conduits as pulmonary conduit replacement unit in sheep:

Three PGG-DBJV tricuspid conduits were implanted in sheep: one for a month and two for three months of the follow-up period. Under cardiopulmonary bypass, the native pulmonary valve leaflets and pulmonary artery were resected and replaced with a PGG-treated decellularized bovine jugular vein valved conduit by end-to-end anastomosis. After the surgery, sheep were allowed to recover and housed for one or three months. During this period, they were monitored by ultrasound for the general cardiopulmonary function to determine the evolution of the graft (potential growth) or identify potential complications of the surgery (bleeding, stenosis, regurgitation, dilatation). At the end of the follow-up period, animals were heparinized to prevent post-mortem thrombosis and euthanized with pentobarbital sodium (80–100 mg/kg, IV). The implants were excised, examined for their gross appearance, and subsequently processed for histological and immunohistochemical analysis. All animal surgeries were done in compliance with Institutional Animal Care and Use Committee (IACUC) approved guidance.

2.18 Statistical Analysis:

All *in vitro* experiments were done in replicates of four or more. The data are reported as the Mean ± Standard Deviation. Data from different groups were analyzed by one-way analysis of variance (ANOVA) followed by Tukey's HSD. All statistical analysis was done using JMP® Pro 15.2.0. Statistical significance and their corresponding significance levels ($p<0.1$, $p<0.05$ or $p<0.01$) were reported for each result.

3. Results:

3.1 Preparation of decellularized scaffolds:

Native bovine jugular veins (BJV) subjected to decellularization maintained their shape, general appearance, and patency of their tri-leaflet valvular apparatus (Figure 1(A)). The effectiveness of the decellularization procedure was analyzed by measuring the amount of DNA in tissues before and after the process. Native walls (n=5) had a DNA concentration of 983.5 ± 131.8 ng/mg dry weight of tissue, while their decellularized counterpart showed 3.0 ± 0.8 ng of DNA/mg dry weight, demonstrating a statistically significant 99.6% reduction in DNA content. Leaflets (n=5) showed a similar significant 99.2% reduction in DNA content, decreasing from 1681.2 ± 84.9 ng DNA/mg dry weight in the native leaflets to 12.3 ± 0.2 ng DNA/mg dry weight in the decellularized samples (Figure 1(B)). Removal of the cellular component was further validated by histological analysis (Figure 1(C)) and agarose gel electrophoresis (Figure S1). DAPI staining of native and decellularized wall and leaflet sections showed the absence of any nuclear staining in the decellularized samples compared to the native tissues. H&E and Masson's trichrome staining did not reveal any difference in the general arrangement and structure of the extracellular matrix before and after the decellularization. In particular, the distribution and arrangement of elastin fibers were similar, as determined by VVG staining (Figure 1(D)).

3.2 Stability of tissues against enzyme degradation:

Since the PGG stabilized BJV conduits are intended to be used as alternatives for the currently used glutaraldehyde fixed conduit replacements, glutaraldehyde fixed native BJV were included as controls in the enzyme challenge assays. During the collagenase challenge assay (n=5), glutaraldehyde-treated samples showed weight loss (6.4 ± 3.6%) significantly lower than the native and decellularized samples (72–96% weight loss). Decellularized 0.05% PGG treated samples, which demonstrated a weight loss of 41.4 ± 28.3%, were significantly less than the native and decellularized samples but significantly more than the glutaraldehyde samples. With an increase in the PGG concentration to 0.15%, the weight loss values significantly decreased, reaching the level of the glutaraldehyde samples. Further increase in PGG concentration, up to 3.33%, did not show statistically significant changes in weight loss compared to the 0.15% PGG treated samples (Figure 2(A)).

The Elastase challenge (n=5) showed a similar trend in the PGG-treated sample groups. The 0.05% PGG-treated samples registered a 25.7 ± 3.3% weight loss, which was significantly lower than values in the native samples. Increasing the PGG concentration to 0.15% significantly reduced the weight loss, reaching a 12.1 ± 3.4% level. A further increase in PGG concentration in the 0.25% −3.33% range did not result in a further significant decrease in weight loss. The glutaraldehyde-fixed samples, with a weight loss of 24.2%, lost significantly less weight compared to the native samples but significantly more compared to the PGG-treated samples within the 0.15%−3.33% concentration range (Figure 2(B)). Increased resistance of the 0.15% PGG-treated samples to elastase enzyme during the digestion process was validated by VVG staining. When comparing the staining pattern before and after elastase treatment, only the PGG-treated samples showed preservation of the elastin fibers present before the treatment (Figure 2(C)).

To evaluate long-term storage potential, 0.15% PGG-treated BJV were stored in PBS for 0, 6, 9, 13, 16, and 24 months and assessed for PGG content and enzyme resistance. After the storage periods, the extraction and quantification of PGG from the samples revealed a PGG content in the range of 28.8 μg/ mg to 55.5 μg/ mg. These values were significantly higher compared to the decellularized tissues; however, no statistically significant difference was observed between the freshly prepared PGG-DBJVC and the stored PGG-treated groups, suggesting that PGG remained bound to the tissue after stabilization for up to 24 months (Figure 2(D)). There was no significant difference between the % dry weight losses among the freshly prepared PGG-treated BJV and those stored for up to 24 months in sterile PBS with Pen/Strep at 4°C, suggesting that the protective effect of the PGG over the extracellular matrix is stable for up to two years of storage (Figure 2(E)).

3.3 Biomechanical characterization of PGG-treated decellularized BJV conduits:

Native, glutaraldehyde fixed native, DBJVC, and PGG-DBJVC wall segments were assessed for their mechanical properties by suture pull out test and biaxial tensile testing.

Maximum force in the longitudinal direction during the suture retention test for glutaraldehyde-fixed, decellularized and PGG treated samples demonstrated statistically comparable levels of average force for failure as the native tissues. Similar force values were registered in the circumferential direction, showing no significant difference between the groups (Figure 3(A)). For the sample elongation during the test, the only statistically significant difference was recorded between native and PGG-treated samples in the circumferential direction (Figure 3(B)). The compliance was calculated and expressed as the maximum force/stretch ratio. A similar trend was observed in the compliance; the glutaraldehyde-fixed, decellularized, and PGG-treated samples were comparable to the native tissues without any statistically significant differences (Figure 3(C)).

During biaxial tensile testing, PGG-DBJVC wall tissues were found to have comparable biomechanical strength as clinically used glutaraldehyde-fixed conduits in both directions. Like the suture retention test, decellularized, PGG-treated, and glutaraldehyde-fixed samples demonstrated comparable stress values at 100% strain as the native tissues without any statistically significant difference (Figure 3(D)). PGG-treated decellularized samples demonstrated a slight stiffening in both directions, recorded in the first half of stretching (Figure 3(I)). The Young's modulus values, calculated within the physiologically relevant range of 10–20% strain, did not show any statistically significant difference between the native, glutaraldehyde-fixed, decellularized, and PGG-treated decellularized tissues (Figure 3(E)).

3.4 Biocompatibility testing:

3.4.1 Cytotoxicity: There was mild biological reactivity (Grade 2) of the cells exposed to the PGG-DBJVC extract (Figure S3). The response obtained from the positive and negative control article extracts confirmed the suitability of the test system. Based on the protocol criteria and the ISO 10993–5 guidelines, the test article met the test requirements and was not considered to have a cytotoxic effect.

3.4.2 Intracutaneous Injection: None of the animals exhibited overt signs of toxicity at any of the observation points. The sites injected with the PGG-DBJVC extract did not show a significantly greater biological reaction than those treated with the control article (Figure S4). The difference in the overall mean score between the test and control articles was 0.0. Based on the criteria of the protocol, the PGG-DBJVC met the requirements of the ISO 10993–10 guidelines.

3.4.3 Sensitization: No systemic signs of toxicity were observed in treated or control animals. None of the treated (NaCl or CSO extracts) or negative control animals exhibited any reaction at the challenge (0% sensitized) (Figure S5). The positive control article elicited discrete reactions in all animals (100% sensitized). The USP 0.9% Sodium Chloride for Injection (NaCl) and Cottonseed Oil (CSO) extracts of the test article, Decell PGG BJV, elicited no reaction at the challenge (0% sensitization) following an induction phase. Therefore, as defined by the grading scale of the USP, the PGG-DBJVC was classified as a non-sensitizer.

3.4.4 Subcutaneous Implantation: Out of the 42 rats implanted subcutaneously with glutaraldehyde-fixed and PGG-treated wall and leaflet samples, two died during the surgeries (due to anesthetic complications). The remaining 40 rats recovered completely, resulting in 5 samples (replicates) per group for every testing (histology and ICP) at both time points. The rats showed no signs of distress, general or local infection, or irritation during the follow-up periods. At both explant time points, the wall and leaflet samples were recovered with ease without any adhesion formation with the underlying muscular layer.

Masson's Trichrome staining was chosen for the general characterization of the explants due to its ability to distinguish the old, darker blue collagen fibers from the newly synthesized, thinner, lighter blue fibers [44]. Two major differences were identified between the glutaraldehyde-fixed and PGG-treated samples: encapsulation and cellular infiltration. At both time points, glutaraldehyde-fixed implants (wall and leaflets) demonstrated a thick capsule composed of compact collagen fibers surrounding the implanted tissues. Moreover, a very intense cellular infiltration was observed in the subcapsular region at the edge of the tissue. Some degree of cellular infiltration into the tissues might have occurred, although it was difficult to distinguish newly invading cells from the initial cellular components of the tissue in the non-decellularized glutaraldehyde fixed samples (Figure 4(A)). PGG-treated samples, on the other hand, showed minimal capsule formation around the tissues; the newly formed collagen fibers were loose and easy to separate from the implants. Minimal infiltration of inflammatory cells was observed in the capsular region, while infiltration of cells was observed within the tissue (Figure 4(B)). The PGG-treated samples were analyzed through immunofluorescence to determine the type of cells invading the scaffolds. The sections stained positive for CD68 pan-macrophage marker at 30- and 90-day time points. These macrophages proved to be of anti-inflammatory (M2) type, as they showed the presence of a CD163 marker. No CD80 pro-inflammatory macrophage marker presence was observed in the scaffolds.

Additionally, no significant positive staining was observed for CD3 T-cell or CD11c dendritic cell markers at either time points (Figure 5). The semi-quantification of the

immune cell staining has been demonstrated in Figure 5(B). Only CD68 and CD163 staining was significantly higher than the negative staining. Positive staining for CD68, CD163, CD80, CD3, and CD11c antibodies were observed in the capsular region of glutaraldehyde-fixed subcutaneously implanted tissues at 30- and 90-days (Figure S6). The glutaraldehyde explants were not quantified since it was difficult to distinguish between the infiltrating cells and the remnant cellular material within the non-decellularized samples.

Alizarin red staining of the PGG-treated decellularized wall and leaflets portions demonstrated no calcification within the implanted scaffolds, whereas all the glutaraldehyde-fixed tissues had heavy calcification within both the leaflet and wall regions (Figure 4(C)). This finding was confirmed by ICP analysis, where glutaraldehyde implants demonstrated elevated levels of elemental calcium and phosphorous within the tissues, with a progressive increase in calcification. Mineral concentration in the PGG-treated implants did not differ significantly before and after implantation (Figure 4(D)).

3.5 Pulmonary conduit replacement in sheep:

As proof of concept, PGG-treated BJV conduits were implanted in 3 sheep as pulmonary conduit replacement units for a 1–3month follow-up period. There were no surgical complications during or after the surgeries. Echocardiography demonstrated minimal or no regurgitation during the 1–3 months (Figure S7). There were no signs of thrombus formation, tissue overgrowth, or leaflet thickening within the implanted conduit walls or leaflets. These findings were confirmed by the gross view of the explanted scaffolds (Figure 6(A)). Size measurements on the PGG-treated conduits performed before and after the 3-month implants demonstrated an increase in the size of the outer diameter and length by 10%.

Histological analysis of the explanted conduits demonstrated repopulation of the leaflets and wall segments with cells (Figure 6(B)-(H)). Immunofluorescence analysis of the grafts revealed positive staining for the endothelial marker VWF, demonstrating active reendothelization of the lumen and leaflet surface during the implant period (Figure 6(C)). Sections from the conduit wall showed positive staining for fibroblast/myofibroblast markers, including alpha-SMA (Figure 6(F)) and Vimentin (Figure 6(G)), and for HSP-47, a chaperone molecule for collagen synthesis, indicating active collagen synthesis within the tissue (Figure 6(E)). Von Kossa staining revealed no calcification within the conduit wall or leaflets at either time point (Figure 6(D)).

4. Discussion:

Bioprosthetic pulmonary conduit replacements have been traditionally produced from native tissues such as pericardium, sub-intestinal submucosa (SIS), or jugular veins [45]. The main advantages of bovine jugular vein valved conduits are the continuity between the valves and conduits and their ‘off the shelf’ availability in pediatric sizes from 12 to 22 mm in diameter [46]. The valved conduits have a structure similar to typical vein tissues, making them adequate to function in a low-pressure system [47]. Moreover, the distal and proximal ends of the conduits allow for extended reconstructive procedures [48].

An ideal replacement conduit must be strong and supple enough upon implantation, resist rapid degradation, allow cellular infiltration, and display remodeling and growth tendency without causing immunologic or thrombotic complications upon implantation. It has been shown that incomplete graft decellularization may result in severe foreign body reactions directed toward graft leaflets [49]. Three criteria were established to determine sufficient decellularization: less than 50 ng of residual DNA/mg dry weight of the tissue, length of DNA fragments smaller than 200 base pairs (bp), and absence of visible nuclear material on histological sections [50]. With residual DNA contents of 3.0 ± 0.8 ng/mg weight in walls, 12.3 ± 0.2 ng/mg in the leaflets, and the absence of any nuclear material by DAPI or H&E staining, the BJV scaffolds obtained through the protocol presented in this work complied with the above criteria that aim to reduce the antigenic burden of the native tissue and thereby overcome adaptive immune response, demonstrating that optimal decellularization of BJV tissues had been achieved. It should, however, be acknowledged that many antigens are not associated with DNA. Antigens like galactose-alpha-1,3-galactose (α-gal), and Sda found within the ECM [51, 52], pose a major threat to immune response if not properly removed, and must be evaluated. The decellularization process might also damage ECM ultrastructure and deplete favorable entities for scaffold functional and regenerative properties [53, 54]. Collagen damage during decellularization might expose cryptic antigenic sites triggering antibody production [55]. Elastin denaturation during decellularization might also produce elastin particles with significant antigenicity [56]. Crosslinking strategies are thereby utilized to reduce the immunogenicity after decellularization by restoring the structural distortions that might have occurred during the process [18]. Although the PGG-DBJVC utilized in this study showed no signs of an elevated inflammatory response, ECM-associated antigen removal needs to be evaluated in future studies.

When implanting a replacement graft, it is desirable for the mechanical properties of the implanted graft to closely approximate those of the native tissue being replaced [45]. The tensile strength of the human pulmonary artery ranges 0.95 ± 0.37 MPa, while the strain at failure is reported to be at 1.61 ± 0.52 mm/mm [57]. The parameters recorded during the suture retention and biaxial tensile testing of the PGG-treated decellularized BJV satisfy these criteria. No statistically significant difference was observed in maximum stress or strain at failure when comparing PGG-treated samples with native and glutaraldehyde-fixed samples. It is important to note that the ultimate stress or strength is not the only characteristic of a replacement graft. A non-linear behavior under load characterizes vascular tissues. Elastin extends at minimal load at lower pressures, while collagen uncrimps and loses its corrugations. As the pressure increases, the load-bearing capability shifts from elastin to collagen, which then becomes the main rigid structural element to resist force [58]. The stress-strain curve computed during the biaxial tensile testing revealed a slight stiffening of the PGG-DBJVC samples during the initial elastic phase of the curve, where slightly higher stress values were recorded at a similar strain compared to the other tested samples. This stiffening was probably due to the PGG's binding to the elastin fibers, fixing them in their wavy state and making them harder to unfold and stretch. Although this stiffening did not reach statistically significant levels during the biaxial testing, significant changes to this non-linear response might alter conduit performance, resulting in life-threatening complications [58, 59]. Since the discussed PGG-DBJVC conduit is a tissue-engineered

conduit, shown to allow cellular infiltration and signs of remodeling at an early stage, further *in vitro* dynamic testing, modeling, and *in-vivo* implantation experiments are required to determine the clinical relevance of these changes and the exact extent of its influence on the hydrodynamic performance of these conduits under physiological conditions. If such stiffening causes significant changes to the hemodynamics of the conduit, the PGG concentration for crosslinking need to be optimized. The glutaraldehyde-fixed samples showed similar elastic behavior to the native samples since glutaraldehyde does not have a cross-linking effect on the elastin fibers but only on the collagen fibers.

In addition to mechanical behavior, the stability of the extracellular matrix elements, particularly elastin, and collagen, and their resistance to enzymatic degradation are essential for the long-term durability of the graft after implantation. Particularly for tissue-engineered grafts, the equilibrium between scaffold degradation and neo-tissue formation is required to render the graft a true regenerative growth potential. The current biomechanical studies on native and glutaraldehyde-fixed samples showed similar mechanical properties, with varying susceptibilities to elastase and collagenase degradation. While no-degradation in glutaraldehyde-treated scaffolds renders them incapable of remodeling, rapid degradation might lead to failure and adverse events after implantation [12, 60]. Different enzyme challenge experiments demonstrated that treatment with PGG of concentrations ≥ 0.15% provided sufficient stabilization of the ECM components, making them resistant to rapid degradation by collagenase and elastase. Future studies will investigate the in vivo degradation rate with different concentrations and evaluate it with the rate of formation of neo-tissue formed after implantation.

When comparing all the examined tissue types in this study, the glutaraldehyde-fixed BJV tissues demonstrated optimal resistance to collagenase digestion but failed to resist rapid degradation by elastase. This finding demonstrates the selective collagen crosslinking capability of glutaraldehyde and provides another insight into the failure of glutaraldehyde-fixed grafts over time [61].

In order to be used as an easily accessible, off-the-shelf device, it is important for the replacement conduits to maintain their properties after extended periods of storage. The long-term storage experiment from this study indicated that even after storage for up to 2 years, the protective effect of the PGG on the extracellular matrix was stable. There was no significant loss of PGG from the scaffolds, and the extracted amount of PGG from tissues did not differ significantly between the freshly prepared samples and those stored for up to 2 years. Moreover, the elastase enzyme challenge of PGG-treated samples from different time points of the 2-year storage period did not show significantly different results between the samples.

Calcification and stenosis in implanted pulmonary valved conduits constitute a substantial concern for pediatric patients. Glutaraldehyde-fixed xenografts and allograft tissues are prone to failure due to calcification and accelerated immune response upon implantation, particularly in pediatric patients [62–66]. Many studies have looked at the anti-calcification treatment of glutaraldehyde-fixed tissues to reduce calcification after implantation [60, 67]. However, the long-term results of these treatments remain to be seen. Decellularization

has been shown to reduce calcification in both homograft and xenograft tissues [68]. Subcutaneous implantation in rats is an established procedure to determine biocompatibility and susceptibility to the calcification of biomaterials [60, 69–70]. Biocompatibility is assessed by the formation of a capsule around the implant, the invasion of cells into the implant, and the characteristics of these invading cells. PGG-DBJVC samples were biocompatible, as demonstrated by the absence of extensive capsule formation and inflammatory cell infiltration around the implants. Cells infiltrating the implants did not show acute or chronic inflammatory cell characteristics. They stained positive for the CD68 pan macrophage marker, and when analyzed further for macrophage subtype, there was much higher levels of CD163 signal, an anti-inflammatory (M2) type macrophage marker compared to CD80, a marker for pro-inflammatory (M1) macrophages. No significant numbers of other inflammatory cell types were seen by 90 days of implantation. Sections showed a virtual absence of positive staining for CD3 T-cell and CD11c dendritic cell markers within the implants. By 90 days post-implantation, some neo-vasculature formation was observed, indicating active remodeling. No signs of calcification were seen in any type (wall or leaflet) of PGG-treated samples at any time. Studies have shown that decellularization prevents the calcification of porcine aortic leaflet tissues, while calcification of decellularized porcine carotid arterial walls has been observed in subcutaneous implantations [71]. This study showed that PGG treatment of the decellularized tissues was shown to resist calcification in the leaflet and wall samples.

Compared to PGG-treated samples, glutaraldehyde-fixed BJV samples showed inferior biocompatibility with extensive calcification that intensified from 1-month to 3-month post-implantation. It has been suggested that the principal regions of calcification are the native cells present within the implanted tissues [72]. Previous studies with PGG treated non-decellularized tissues have shown the potential of PGG treatment to reduce calcification in subcutaneously implanted tissues, including calcification reduction when combined with glutaraldehyde treatment [24, 73]. The PGG-DBJVC tissues in this study were shown to completely resist calcification for up to 3 months, further demonstrating the ability of PGG to protect the implants after implantation. It should, however, be acknowledged that the glutaraldehyde treatment process used in this study was adapted from literature and is not identical to that used in current clinically implanted devices. For a further evaluation of the anti-calcification potential of the PGG-DBJVC, they need to be compared to the commercially available products that are currently available.

Our proof-of-concept sheep implant studies demonstrated the feasibility of PGG-treated decellularized BJV scaffolds for replacement conduits in the pulmonary position. At both time points, the conduits remained patent with normal hemodynamical parameters. There were no signs of stenosis or regurgitation, and the leaflets functioned normally. Histological analysis showed infiltration of cellular components within the decellularized PGG-DBJVC. Most of these infiltrated cells were determined to be fibroblast and myofibroblast-like cells with little inflammatory cells.

Additionally, the explanted tissues demonstrated the presence of HSP-47 within the grafts. HSP-47 is a chaperon molecule implicated in collagen synthesis and, together with the fibroblast/myofibroblast characteristics of the infiltrating cells, a strong indicator of active

remodeling within the scaffolds [74–76]. Cellular infiltration and remodeling of the implants is an essential feature of the scaffolds' capacity to grow with the patients. Cardiovascular devices that lack an endothelial lining or fail to get reendothelized upon implantation are prone to platelet aggregation and thrombus formation [77, 78], and patients receiving such a device require lifelong anticoagulant therapy, diminishing the quality of life of a pediatric patient. In the sheep implantation model, the PGG-DBJVC showed an endothelial cell lining along their luminal side, potentially protecting thrombotic events after implantation. Enlargement of the graft by ten percent was observed, but with the small number of animals used in this study, it cannot be claimed with certainty that this enlargement represented the actual regenerative growth of the device.

Additionally, although the sheep implant studies demonstrated repopulation of the implants with non-inflammatory cells and the presence of HSP-47, further analysis needs to be conducted to evaluate collagen turnover, neo-collagen formation, and the TIMP and MMP profiles within the implants to demonstrate implant remodeling. Future large-animal studies will aim to increase the number of animals with an extended follow-up period at each time point, along with clinically used controls to evaluate the performance of the conduit. Biomechanical data will be collected in vivo and computationally modeled to monitor in-vivo growth of the conduit after implantation. Additionally, analysis of the proteomic distribution within the PGG-DBJVC, before and after implantation, will reveal vital information on the remodeling potential of these grafts.

5. Conclusions:

We have successfully demonstrated the feasibility of the unique combinatory method for developing an improved replacement conduit using decellularized bovine jugular veins stabilized with PGG. The PGG-treated conduits met all the criteria for an optimal replacement conduit, including adequate biomechanical strength, resistance to degradation, remodeling, and absence of adverse inflammatory responses, calcification, or thrombotic events. We focused on developing an ideal valved conduit that is durable and grows with the patient is particularly promising, as this could reduce or eliminate the need for reinterventions in pediatric patients. This work represents a significant step forward in tissue engineering and could have major implications for treating patients requiring replacement conduits. However, it should be noted that further research will be necessary to evaluate fully the safety and efficacy of this approach and to determine the long-term outcomes for patients who receive PGG-treated decellularized conduits.

Supplementary Material

Refer to Web version on PubMed Central for supplementary material.

Acknowledgments:

We greatly appreciate help from the core facilities of the SCBioCRAFT center at Clemson University.

Funding:

This work was supported by STTR Phase I Grant from the National Institute of Health (NIH) [R41HL147771, 2019].

Abbreviations:

ANOVA	Analysis of Variance
BJV	Bovine Jugular Vein
CD	Cluster of Differentiation
CDRH	Center for Devices and Radiological Health
CFR	Code of Federal Regulation
CHD	Congenital Heart Disease
CSO	Cotton Seed Oil
DAPI	4’, 6- diamidino- 2-phenylindole
DBJVC	Decellularized Bovine Jugular Vein Conduit
DNA	Deoxyribonucleic acid
DOC	sodium Deoxycholate
dsDNA	double stranded Deoxyribonucleic acid
ECM	Extra cellular matrix
EDTA	Ethylene Diamine Tetra-Acetic acid
ETVGs	Elastin-rich tubular vascular grafts
F-C Reagent	Folin-Ciocalteu
FDA	U.S. Food and Drug Administration
GLP	Good Laboratory Practice
Glut	Glutaraldehyde
H&E	Hematoxylin and Eosin
HCL	Hydrochloric Acid
HEPES	2-[4-(2-hydroxyethyl) piperazin-1-yl] ethane sulfonic acid
HSD	Honestly Significant Difference
HSP-47	Heat Shock Protein-47
IACUC	institutional animal care and use committee

ICP	Inductively Coupled Plasma
IHC	Immuno-Histo Chemistry
ISO	International Organization of Standards
NaOH	Sodium hydroxide
NIH	National Institute of Health
NMR	Nuclear Magnetic Resonance
PBS	Phosphate Buffered Saline
PGG	Pentagalloyl Glucose
PGG-DBJVC	PGG treated decellularized bovine jugular vein conduit
RNA	Ribonucleic Acid
RVOT	Right Ventricular Outflow Tract
SD	Sprague Dawley
SIS	Small Intestinal Submucosa
SMA	Smooth Muscle Actin
STTR	Small Business Technology Transfer
TRIS	tris (hydroxymethyl) amino-methane
USDA	United States Department of Agriculture
USP	United States Pharmacopeia
VWF	von Willebrand factor
VVG	Verhoeff-Van Gieson

References:

[1]. van der Bom T, Zomer AC, Zwinderman AH, Meijboom FJ, Bouma BJ, Mulder BJ. The changing epidemiology of congenital heart disease. Nat Rev Cardiol. 2011 Jan;8(1):50–60. doi: 10.1038/nrcardio.2010.166. [PubMed: 21045784]

[2]. Greutmann M. Tetralogy of Fallot, pulmonary valve replacement, and right ventricular volumes: are we chasing the right target? Eur Heart J. 2016 Mar 7;37(10):836–9. doi: 10.1093/eurheartj/ehv634. [PubMed: 26685132]

[3]. Ciaravella JM Jr, McGoon DC, Danielson GK, Wallace RB, Mair DD, Ilstrup DM. Experience with the extracardiac conduit. J Thorac Cardiovasc Surg. 1979 Dec;78(6):920–30. [PubMed: 159385]

[4]. Ong K, Boone R, Gao M, Carere R, Webb J, Kiess M, Grewal J. Right ventricle to pulmonary artery conduit reoperations in patients with tetralogy of fallot or pulmonary atresia associated with ventricular septal defect. Am J Cardiol. 2013 Jun 1;111(11):1638–43. doi: 10.1016/j.amjcard.2013.01.337. [PubMed: 23481618]

[5]. van Steenberghe M, Schubert T, Gerelli S, Bouzin C, Guiot Y, Xhema D, Bollen X, Abdelhamid K, Gianello P. Porcine pulmonary valve decellularization with NaOH-based vs detergent process: preliminary in vitro and in vivo assessments. J Cardiothorac Surg 13, 34 (2018). 10.1186/s13019-018-0720-y [PubMed: 29695259]

[6]. Ruel M, Chan V, Bédard P, Kulik A, Ressler L, Lam BK, Rubens FD, Goldstein W, Hendry PJ, Masters RG, Mesana TG. Very long-term survival implications of heart valve replacement with tissue versus mechanical prostheses in adults <60 years of age. Circulation. 2007 Sep 11;116(11 Suppl):I294–300. doi: 10.1161/CIRCULATIONAHA.106.681429. [PubMed: 17846320]

[7]. Kim DJ, Kim YJ, Kim WH, Kim SH. Xenograft Failure of Pulmonary Valved Conduit Cross-linked with Glutaraldehyde or Not Cross-linked in a Pig to Goat Implantation Model. Korean J Thorac Cardiovasc Surg. 2012 Oct;45(5):287–94. doi: 10.5090/kjtcs.2012.45.5.287. [PubMed: 23130301]

[8]. Gist KM, Mitchell MB, Jaggers J, Campbell DN, Yu JA, Landeck BF 2nd. Assessment of the relationship between Contegra conduit size and early valvar insufficiency. Ann Thorac Surg. 2012 Mar;93(3):856–61. doi: 10.1016/j.athoracsur.2011.10.057. [PubMed: 22300627]

[9]. Nichay NR, Zhuravleva IY, Kulyabin YY, Timchenko TP, Voitov AV, Kuznetsova EV, Soynov IA, Zubritskiy AV, Bogachev-Prokophiev AV, Karaskov AM. In search of the best xenogeneic material for a paediatric conduit: an analysis of clinical data. Interact Cardiovasc Thorac Surg. 2018 Jul 1;27(1):34–41. doi: 10.1093/icvts/ivy029. [PubMed: 29452369]

[10]. Center for Devices and Radiological Health, (CDRH), Medtronic Contegra® Pulmonary Valved Conduit, Center for Devices and Radiological Health, e September 12, 2017.

[11]. Simon P, Kasimir MT, Seebacher G, Weigel G, Ullrich R, Salzer-Muhar U, Rieder E, Wolner E. Early failure of the tissue engineered porcine heart valve SYNERGRAFT in pediatric patients. Eur J Cardiothorac Surg. 2003 Jun;23(6):1002–6; discussion 1006. doi: 10.1016/s1010-7940(03)00094-0. [PubMed: 12829079]

[12]. van Rijswijk JW, Talacua H, Mulder K, van Hout GPJ, Bouten CVC, Gründeman PF, Kluin J. Failure of decellularized porcine small intestinal submucosa as a heart valved conduit. J Thorac Cardiovasc Surg. 2020 Oct;160(4):e201–e215. doi: 10.1016/j.jtcvs.2019.09.164. [PubMed: 32151387]

[13]. Rüffer A, Purbojo A, Cicha I, Glöckler M, Potapov S, Dittrich S, Cesnjevar RA. Early failure of xenogenous de-cellularised pulmonary valve conduits--a word of caution! Eur J Cardiothorac Surg. 2010 Jul;38(1):78–85. doi: 10.1016/j.ejcts.2010.01.044. [PubMed: 20219384]

[14]. Morales DL, Herrington C, Bacha EA, Morell VO, Prodán Z, Mroczek T, Sivalingam S, Cox M, Bennink G, Asch FM. A Novel Restorative Pulmonary Valve Conduit: Early Outcomes of Two Clinical Trials. Front Cardiovasc Med. 2021 Mar 4;7:583360. doi: 10.3389/fcvm.2020.583360.

[15]. Prodan Z, Mroczek T, Sivalingam S, Bennink G, Asch FM, Cox M, Carrel T; Xeltis BVWorking Group; Yakub MA, Nagy Z, Skalski J, Svanidze O, Schutte E, Verhees L, Klersy C, Virmani R, Sreeram N. Initial Clinical Trial of a Novel Pulmonary Valved Conduit. Semin Thorac Cardiovasc Surg. 2022 Autumn;34(3):985–991. doi: 10.1053/j.semtcvs.2021.03.036.

[16]. Avolio E, Caputo M, Madeddu P. Stem cell therapy and tissue engineering for correction of congenital heart disease. Front Cell Dev Biol. 2015 Jun 30;3:39. doi: 10.3389/fcell.2015.00039. [PubMed: 26176009]

[17]. Ma B, Wang X, Wu C, Chang J. Crosslinking strategies for preparation of extracellular matrix-derived cardiovascular scaffolds. Regen Biomater. 2014 Nov;1(1):81–9. doi: 10.1093/rb/rbu009.

[18]. Kasravi M, Ahmadi A, Babajani A, Mazloomnejad R, Hatamnejad MR, Shariatzadeh S, Bahrami S, Niknejad H. Immunogenicity of decellularized extracellular matrix scaffolds: a bottleneck in tissue engineering and regenerative medicine. Biomater Res. 2023 Feb 9;27(1):10. doi: 10.1186/s40824-023-00348-z. [PubMed: 36759929]

[19]. Luck G, Liao H, Murray NJ, Grimmer HR, Warminski EE, Williamson MP, Lilley TH, Haslam E. Polyphenols, astringency and proline-rich proteins. Phytochemistry. 1994 Sep;37(2):357–71. doi: 10.1016/0031-9422(94)85061-5. [PubMed: 7765619]

[20]. Charlton AJ, Baxter NJ, Lilley TH, Haslam E, McDonald CJ, Williamson MP. Tannin interactions with a full-length human salivary proline-rich protein display a stronger affinity than with single proline-rich repeats. FEBS Lett. 1996 Mar 18;382(3):289–92. doi: 10.1016/0014-5793(96)00186-x. [PubMed: 8605987]

[21]. Baxter NJ, Lilley TH, Haslam E, Williamson MP. Multiple interactions between polyphenols and a salivary proline-rich protein repeat result in complexation and precipitation. Biochemistry. 1997 May 6;36(18):5566–77. doi: 10.1021/bi9700328. [PubMed: 9154941]

[22]. Pavey SN, Cocciolone AJ, Marty AG, Ismail HN, Hawes JZ, Wagenseil JE. Pentagalloyl glucose (PGG) partially prevents arterial mechanical changes due to elastin degradation. Exp Mech. 2021 Jan;61(1):41–51. doi: 10.1007/s11340-020-00625-1. [PubMed: 33746235]

[23]. Sinha A, Nosoudi N, Vyavahare N. Elasto-regenerative properties of polyphenols. Biochem Biophys Res Commun. 2014 Feb 7;444(2):205–11. doi: 10.1016/j.bbrc.2014.01.027. [PubMed: 24440697]

[24]. Isenburg JC, Simionescu DT, Vyavahare NR. Tannic acid treatment enhances biostability and reduces calcification of glutaraldehyde fixed aortic wall. Biomaterials. 2005 Apr;26(11):1237–45. doi: 10.1016/j.biomaterials.2004.04.034. [PubMed: 15475053]

[25]. Rosenbloom J, Abrams WR, Mecham R (1993), Extracellular matrix 4: The elastic fiber. The FASEB Journal, 7: 1208–1218. 10.1096/fasebj.7.13.8405806 [PubMed: 8405806]

[26]. Cao Y, Himmeldirk KB, Qian Y, Ren Y, Malki A, Chen X. Biological and biomedical functions of Penta-O-galloyl-D-glucose and its derivatives. J Nat Med. 2014 Jul;68(3):465–72. doi: 10.1007/s11418-014-0823-2. [PubMed: 24532420]

[27]. Torres-León C, Ventura-Sobrevilla J, Serna-Cock L, Ascacio-Valdés JA, Contreras-Esquivel J, Aguilar CN. Pentagalloylglucose (PGG): A valuable phenolic compound with functional properties. Journal of Functional Foods. 2017 Oct 1;37:176–89.

[28]. Zhang J, Li L, Kim SH, Hagerman AE, Lü J. Anti-cancer, anti-diabetic and other pharmacologic and biological activities of penta-galloyl-glucose. Pharm Res. 2009 Sep;26(9):2066–80. doi: 10.1007/s11095-009-9932-0. [PubMed: 19575286]

[29]. Lu Q, Ganesan K, Simionescu DT, Vyavahare NR. Novel porous aortic elastin and collagen scaffolds for tissue engineering. Biomaterials. 2004 Oct;25(22):5227–37. doi: 10.1016/j.biomaterials.2003.12.019. [PubMed: 15110474]

[30]. Simionescu DT, Lu Q, Song Y, Lee JS, Rosenbalm TN, Kelley C, Vyavahare NR. Biocompatibility and remodeling potential of pure arterial elastin and collagen scaffolds. Biomaterials. 2006 Feb;27(5):702–13. doi: 10.1016/j.biomaterials.2005.06.013. [PubMed: 16048731]

[31]. Sinha D, “Development of Tissue Engineered Scaffolds for Cardiovascular Repair and Replacement in Pediatric Patients” (2021). All Dissertations. 2940. https://tigerprints.clemson.edu/all_dissertations/2940

[32]. Tam H, Zhang W, Feaver KR, Parchment N, Sacks MS, Vyavahare N. A novel crosslinking method for improved tear resistance and biocompatibility of tissue based biomaterials. Biomaterials. 2015 Oct;66:83–91. doi: 10.1016/j.biomaterials.2015.07.011. [PubMed: 26196535]

[33]. Rosenblatt M, Peluso JV, Determination of Tannins by Photocolorimeter, Journal of Association of Official Agricultural Chemists, Volume 24, Issue 1, 1 February 1941, Pages 170–181, 10.1093/jaoac/24.1.170

[34]. Singleton VL, Orthofer R, Lamuela-Raventós RM. [14] Analysis of total phenols and other oxidation substrates and antioxidants by means of folin-ciocalteu reagent. In Methods in enzymology 1999 Jan 1 (Vol. 299, pp. 152–178). Academic press.

[35]. Simionescu D, Casco M, Turner J, Rierson N, Yue J, Ning K. Chemical stabilization of the extracellular matrix attenuates growth of experimentally induced abdominal aorta aneurysms in a large animal model. JVS Vasc Sci. 2020 Apr 23;1:69–80. doi: 10.1016/j.jvssci.2020.04.001. [PubMed: 34617039]

[36]. International Standard Organization, Cardiovascular implants and extracorporeal systems - Vascular prostheses - Tubular vascular grafts and vascular patches (ISO 7198:2016), Jul, 2017.

[37]. Pensalfini M, Meneghello S, Lintas V, Bircher K, Ehret AE, Mazza E. The suture retention test, revisited and revised. J Mech Behav Biomed Mater. 2018 Jan;77:711–717. doi: 10.1016/j.jmbbm.2017.08.021. [PubMed: 28867371]

[38]. Lu Q. Evaluation of arterial elastin and collagen scaffolds for cardiovascular tissue engineering. Clemson University; 2005.

[39]. Huang HS, Lu J. Biaxial mechanical properties of bovine jugular venous valve leaflet tissues. Biomech Model Mechanobiol. 2017 Dec;16(6):1911–1923. doi: 10.1007/s10237-017-0927-1. [PubMed: 28631145]

[40]. Davis FM, De Vita R. A nonlinear constitutive model for stress relaxation in ligaments and tendons. Ann Biomed Eng. 2012 Dec;40(12):2541–50. doi: 10.1007/s10439-012-0596-2. [PubMed: 22648576]

[41]. Tam H. (2016). Novel chemical crosslinking to stabilize extracellular matrix for bioprosthetic heart valve materials to resist calcification and structural degradation.

[42]. Schindelin J, Arganda-Carreras I, Frise E, Kaynig V, Longair M, Pietzsch T, Preibisch S, Rueden C, Saalfeld S, Schmid B, Tinevez JY, White DJ, Hartenstein V, Eliceiri K, Tomancak P, Cardona A. Fiji: an open-source platform for biological-image analysis. Nat Methods. 2012 Jun 28;9(7):676–82. doi: 10.1038/nmeth.2019. [PubMed: 22743772]

[43]. Crowe AR, Yue W. Semi-quantitative Determination of Protein Expression using Immunohistochemistry Staining and Analysis: An Integrated Protocol. Bio Protoc. 2019 Dec 20;9(24):e3465. doi: 10.21769/BioProtoc.3465.

[44]. Boennelycke M, Christensen L, Nielsen LF, Everland H, Lose G. Tissue response to a new type of biomaterial implanted subcutaneously in rats. Int Urogynecol J. 2011 Feb;22(2):191–6. doi: 10.1007/s00192-010-1257-3. [PubMed: 20838988]

[45]. Manavitehrani I, Ebrahimi P, Yang I, Daly S, Schindeler A, Saxena A, Little DG, Fletcher DF, Dehghani F, Winlaw DS. Current Challenges and Emergent Technologies for Manufacturing Artificial Right Ventricle to Pulmonary Artery (RV-PA) Cardiac Conduits. Cardiovascular Engineering and Technology. 2019 Jun;10(2):205–215. DOI: 10.1007/s13239-019-00406-5. [PubMed: 30767113]

[46]. Rastan AJ, Walther T, Daehnert I, Hambsch J, Mohr FW, Janousek J, Kostelka M. Bovine jugular vein conduit for right ventricular outflow tract reconstruction: evaluation of risk factors for mid-term outcome. Ann Thorac Surg. 2006 Oct;82(4):1308–15. doi: 10.1016/j.athoracsur.2006.04.071. [PubMed: 16996925]

[47]. Ichikawa Y, Noishiki Y, Kosuge T, Yamamoto K, Kondo J, Matsumoto A. Use of a bovine jugular vein graft with natural valve for right ventricular outflow tract reconstruction: a one-year animal study. J Thorac Cardiovasc Surg. 1997 Aug;114(2):224–33. doi: 10.1016/S0022-5223(97)70149-1. [PubMed: 9270640]

[48]. Fiore AC, Ruzmetov M, Huynh D, Hanley S, Rodefeld MD, Turrentine MW, Brown JW. Comparison of bovine jugular vein with pulmonary homograft conduits in children less than 2 years of age. Eur J Cardiothorac Surg. 2010 Sep;38(3):318–25. doi: 10.1016/j.ejcts.2010.01.063. [PubMed: 20356755]

[49]. Hiemann NE, Mani M, Huebler M, Meyer R, Hetzer R, Thieme R, Bethge C. Complete destruction of a tissue-engineered porcine xenograft in pulmonary valve position after the Ross procedure. J Thorac Cardiovasc Surg. 2010 Apr;139(4):e67–8. doi: 10.1016/j.jtcvs.2008.12.033. [PubMed: 19660290]

[50]. Faulk DM, Johnson SA, Badylak SF. Decellularized biological scaffolds for cardiac repair and regeneration. In Cardiac regeneration and repair 2014 Jan 1 (pp. 180–200). Woodhead Publishing.

[51]. Zhao C, Cooper DKC, Dai Y, Hara H, Cai Z, Mou L. The Sda and Cad glycan antigens and their glycosyltransferase, β1,4GalNAcT-II, in xenotransplantation. Xenotransplantation. 2018 Mar;25(2):e12386. doi: 10.1111/xen.12386. [PubMed: 29430727]

[52]. Huai G, Qi P, Yang H, Wang Y. Characteristics of α-Gal epitope, anti-Gal antibody, α1,3 galactosyltransferase and its clinical exploitation (Review). Int J Mol Med. 2016 Jan;37(1):11–20. doi: 10.3892/ijmm.2015.2397. [PubMed: 26531137]

[53]. Aamodt JM, Grainger DW. Extracellular matrix-based biomaterial scaffolds and the host response. Biomaterials. 2016 Apr;86:68–82. doi: 10.1016/j.biomaterials.2016.02.003. [PubMed: 26890039]

[54]. White LJ, Taylor AJ, Faulk DM, Keane TJ, Saldin LT, Reing JE, Swinehart IT, Turner NJ, Ratner BD, Badylak SF. The impact of detergents on the tissue decellularization process: A ToF-SIMS study. Acta Biomater. 2017 Mar 1;50:207–219. doi: 10.1016/j.actbio.2016.12.033. [PubMed: 27993639]

[55]. Chakraborty J, Roy S, Murab S, Ravani R, Kaur K, Devi S, Singh D, Sharma S, Mohanty S, Dinda AK, Tandon R, Ghosh S. Modulation of Macrophage Phenotype, Maturation, and Graft Integration through Chondroitin Sulfate Cross-Linking to Decellularized Cornea. ACS Biomater Sci Eng. 2019 Jan 14;5(1):165–179. doi: 10.1021/acsbiomaterials.8b00251. [PubMed: 33405862]

[56]. Mecham RP, Lange G. Antigenicity of elastin: characterization of major antigenic determinants on purified insoluble elastin. Biochemistry. 1982 Feb 16;21(4):669–73. doi: 10.1021/bi00533a013. [PubMed: 6176263]

[57]. Hoerstrup SP, Kadner A, Breymann C, Maurus CF, Guenter CI, Sodian R, Visjager JF, Zund G, Turina MI. Living, autologous pulmonary artery conduits tissue engineered from human umbilical cord cells. Ann Thorac Surg. 2002 Jul;74(1):46–52; discussion 52. doi: 10.1016/s0003-4975(02)03649-4. [PubMed: 12118802]

[58]. Camasão DB, Mantovani D. The mechanical characterization of blood vessels and their substitutes in the continuous quest for physiological-relevant performances. A critical review. Mater Today Bio. 2021 Mar 7;10:100106. doi: 10.1016/j.mtbio.2021.100106.

[59]. Zia AW, Liu R, Wu X. Structural design and mechanical performance of composite vascular grafts. Bio-des. Manuf. 5, 757–785 (2022). 10.1007/s42242-022-00201-7

[60]. Wright GA, Faught JM, Olin JM. Assessing anticalcification treatments in bioprosthetic tissue by using the New Zealand rabbit intramuscular model. Comp Med. 2009 Jun;59(3):266–71. PMID: 19619417; PMCID: PMC2733289. [PubMed: 19619417]

[61]. Isenburg JC, Karamchandani NV, Simionescu DT, Vyavahare NR. Structural requirements for stabilization of vascular elastin by polyphenolic tannins. Biomaterials. 2006 Jul;27(19):3645–51. doi: 10.1016/j.biomaterials.2006.02.016. [PubMed: 16527345]

[62]. Brown JW, Ruzmetov M, Rodefeld MD, Vijay P, Turrentine MW. Right ventricular outflow tract reconstruction with an allograft conduit in non-ross patients: risk factors for allograft dysfunction and failure. Ann Thorac Surg. 2005 Aug;80(2):655–63; discussion 663–4. doi: 10.1016/j.athoracsur.2005.02.053. [PubMed: 16039222]

[63]. Javadpour H, Veerasingam D, Wood AE. Calcification of homograft valves in the pulmonary circulation -- is it device or donation related? Eur J Cardiothorac Surg. 2002 Jul;22(1):78–81. doi: 10.1016/s1010-7940(02)00245-2. [PubMed: 12103377]

[64]. Hopkins R. From cadaver harvested homograft valves to tissue-engineered valve conduits. Progress in Pediatric cardiology. 2006 Mar 1;21(2):137–52.

[65]. Huyan Y, Chang Y, Song J. Application of Homograft Valved Conduit in Cardiac Surgery. Front Cardiovasc Med. 2021 Oct 12;8:740871. doi: 10.3389/fcvm.2021.740871. [PubMed: 34712711]

[66]. Xue Y, Kossar AP, Abramov A, Frasca A, Sun M, Zyablitskaya M, Paik D, Kalfa D, Della Barbera M, Thiene G, Kozaki S, Kawashima T, Gorman JH, Gorman RC, Gillespie MJ, Carreon CK, Sanders SP, Levy RJ, Ferrari G. Age-related enhanced degeneration of bioprosthetic valves due to leaflet calcification, tissue crosslinking, and structural changes. Cardiovasc Res. 2023 Mar 17;119(1):302–315. doi: 10.1093/cvr/cvac002. [PubMed: 35020813]

[67]. Vyavahare N, Tam H. (2018). Bioprosthetic Heart Valves: From a Biomaterials Perspective. In: Sacks M., Liao J (eds) Advances in Heart Valve Biomechanics. Springer, Cham. 10.1007/978-3-030-01993-8_14

[68]. Hopkins RA, Jones AL, Wolfinbarger L, Moore MA, Bert AA, Lofland GK. Decellularization reduces calcification while improving both durability and 1-year functional results of pulmonary homograft valves in juvenile sheep. J Thorac Cardiovasc Surg. 2009 Apr;137(4):907–13, 913e1–4. doi: 10.1016/j.jtcvs.2008.12.009. [PubMed: 19327516]

[69]. Mako WJ, Shah A, Vesely I. Mineralization of glutaraldehyde-fixed porcine aortic valve cusps in the subcutaneous rat model: analysis of variations in implant site and cuspal quadrants. J Biomed Mater Res. 1999 Jun 5;45(3):209–13. doi: 10.1002/(sici)1097-4636(19990605)45:3<209::aid-jbm8>3.0.co;2-n. [PubMed: 10397978]

[70]. Levy RJ, Schoen FJ, Levy JT, Nelson AC, Howard SL, Oshry LJ. Biologic determinants of dystrophic calcification and osteocalcin deposition in glutaraldehyde-preserved porcine aortic valve leaflets implanted subcutaneously in rats. Am J Pathol. 1983 Nov;113(2):143–55. PMID: 6605687; PMCID: PMC1916380. [PubMed: 6605687]

[71]. Chow JP, Simionescu DT, Warner H, Wang B, Patnaik SS, Liao J, Simionescu A. Mitigation of diabetes-related complications in implanted collagen and elastin scaffolds using matrix-binding polyphenol. Biomaterials. 2013 Jan;34(3):685–95. doi: 10.1016/j.biomaterials.2012.09.081. [PubMed: 23103157]

[72]. Badria AF, Koutsoukos PG, Mavrilas D. Decellularized tissue-engineered heart valves calcification: what do animal and clinical studies tell us? J Mater Sci Mater Med. 2020 Dec 5;31(12):132. doi: 10.1007/s10856-020-06462-x. [PubMed: 33278023]

[73]. Tedder ME, Liao J, Weed B, Stabler C, Zhang H, Simionescu A, Simionescu DT. Stabilized collagen scaffolds for heart valve tissue engineering. Tissue Eng Part A. 2009 Jun;15(6):1257–68. doi: 10.1089/ten.tea.2008.0263. [PubMed: 18928400]

[74]. Ishida Y, Nagata K. Hsp47 as a collagen-specific molecular chaperone. Methods Enzymol. 2011;499:167–82. doi: 10.1016/B978-0-12-386471-0.00009-2. [PubMed: 21683254]

[75]. Ito S, Nagata K. Roles of the endoplasmic reticulum-resident, collagen-specific molecular chaperone Hsp47 in vertebrate cells and human disease. J Biol Chem. 2019 Feb 8;294(6):2133–2141. doi: 10.1074/jbc.TM118.002812. [PubMed: 30541925]

[76]. Kim HJ, Park JH, Shin JM, Yang HW, Lee HM, Park IH. TGF-β1-induced HSP47 regulates extracellular matrix accumulation via Smad2/3 signaling pathways in nasal fibroblasts. Sci Rep. 2019 Oct 29;9(1):15563. doi: 10.1038/s41598-019-52064-1. Erratum in: Sci Rep. 2020 Jun 9;10(1):9585. [PubMed: 31664133]

[77]. Yau JW, Teoh H, Verma S. Endothelial cell control of thrombosis. BMC Cardiovasc Disord. 2015 Oct 19;15:130. doi: 10.1186/s12872-015-0124-z. [PubMed: 26481314]

[78]. Wu KK, Thiagarajan P. Role of endothelium in thrombosis and hemostasis. Annu Rev Med. 1996;47:315–31. doi: 10.1146/annurev.med.47.1.315. [PubMed: 8712785]

Statement of Significance

Congenital Heart Disease (CHD) is a common congenital disorder affecting many newborns in the United States each year. The use of substitute conduit arteries is necessary for some patients with CHD who have missing or underdeveloped structures. Current conduit replacement devices have limitations, including stiffness, susceptibility to infection and thrombosis, and lack of implant growth capacity. Pentagalloyl glucose-stabilized bovine jugular vein valved tissue (PGG-DBJVC) offers a promising solution as it is resistant to calcification, and biocompatible. When implanted in rats and as pulmonary conduit replacement in sheep, the PGG-DBJVC demonstrated cellular infiltration without excessive inflammation, which could lead to remodeling and integration with host tissue and eliminate the need for replacement as the child grows.

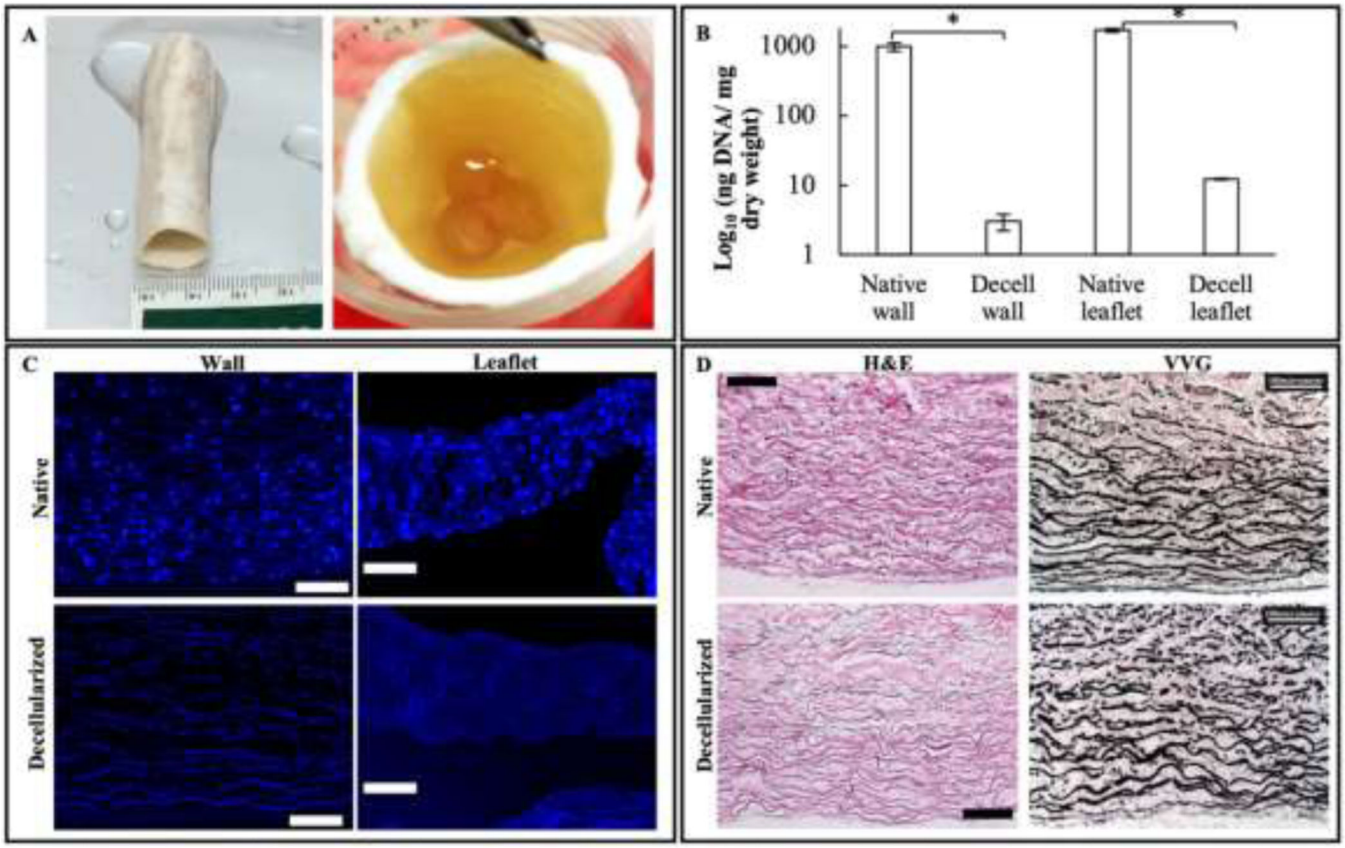

Figure 1:

Preparation of decellularized PGG-treated BJV conduits: (A) Macroscopic view of decellularized PGG-treated bovine jugular vein conduit, with a patent tri-leaflet valve; (B) Residual DNA quantification in native and decellularized (Decell) walls and leaflets, N=5, ng DNA/ mg dry weight expressed as a Log_{10} function; *$p<0.001$; (C) DAPI staining of native and decellularized walls and leaflets, showing complete absence of nuclear material in the decellularized samples (scale bar: 100 μm) (D) H&E and VVG staining of native and decellularized BJV walls showing preservation of extracellular matrix (ECM) after decellularization (scale bar: 100 μm).

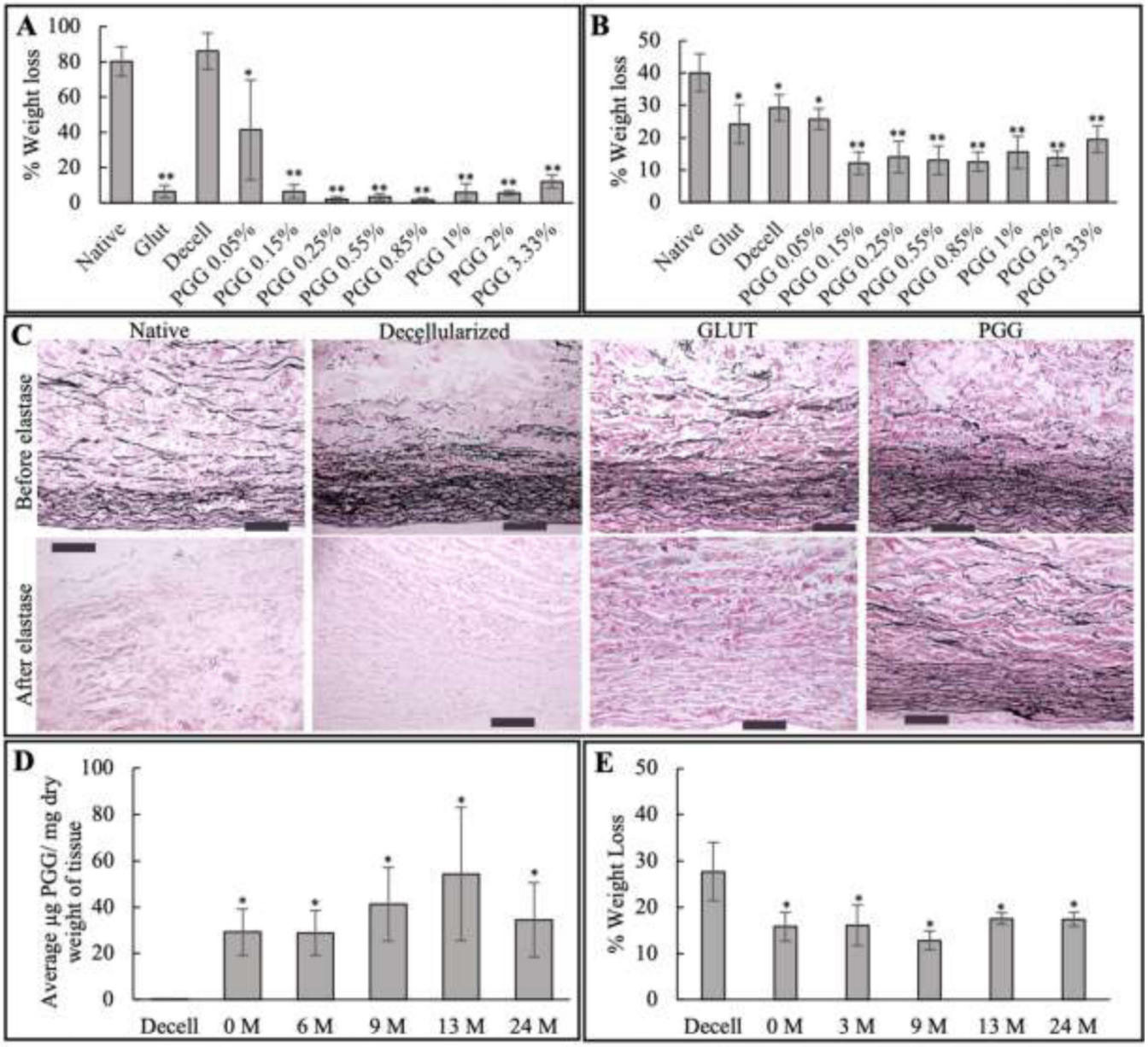

Figure 2:

Stabilization of extracellular matrix in the prepared grafts: (**A**) % weight loss during collagenase treatment; N=5; *p<0.001, significantly reduced compared to native and decellularized (decell) groups; **p<0.001, significantly reduced compared to native, decell, and PGG 0.05% group; (**B**) % weight loss during elastase treatment; N=5; *p<0.001, significantly reduced compared to native group; **p<0.001, significantly reduced compared to native, glutaraldehyde (glut), decellularized (decell), and PGG 0.05% groups (**C**) VVG staining of native, decellularized, glutaraldehyde treated native (Glut), and PGG-treated decellularized (PGG.) BJV before and after treatment with elastase enzyme, showing preservation of elastin only in PGG treated samples (scale bar: 200 µm). (**D**) PGG content, expressed as µg PGG/ mg dry weight, of 0.15% PGG treated bovine jugular vein (BJV)

samples stored for up-to 24-months (0, 6, 9, 13, and 24 months); *p<0.001 Statistically significant difference in PGG concentration compared to decellularized (decell) tissues. No significant difference among groups of different storage time, N=8; (**E**) % weight loss during elastase treatment of 0.15% PGG-treated B.J.V. tissues stored for up-to 24-months (0, 6, 9, 13, and 24 months),* p<0.001, Statistically significant difference compared to decellularized (decell) BJV, No significant difference among groups of different storage time, N=8 to decellularized (decell) BJV, No significant difference among groups of different storage time, N=8

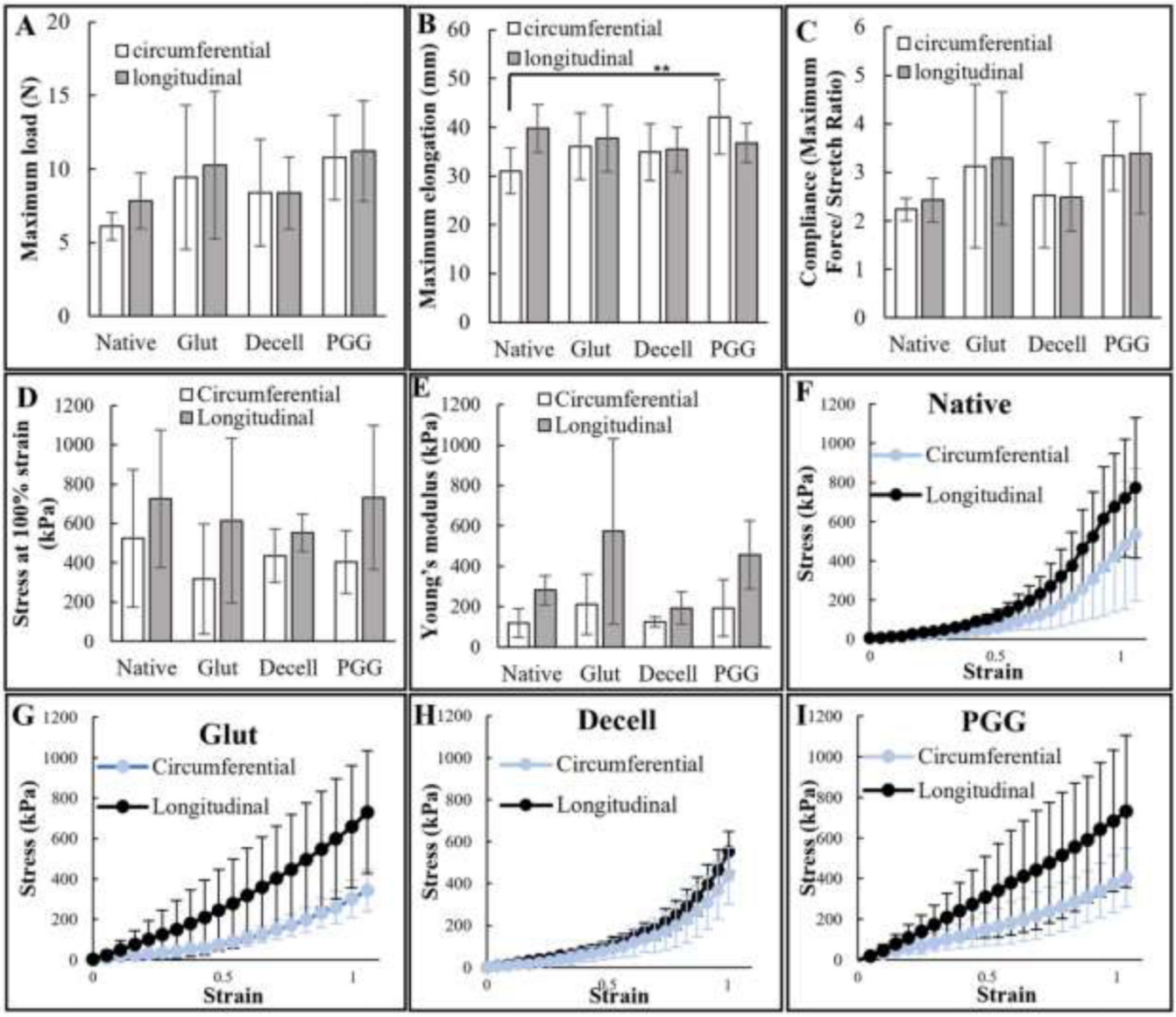

Figure 3:

Mechanical testing of PGG-treated decellularized BJV: (A) Maximum load at failure recorded during suture retention testing, N=6, no significant difference registered between native, glutaraldehyde (glut) treated, decellularized (decell), and PGG treated (PGG) samples in either direction; (B) Maximum elongation recorded during suture retention testing, N=6; only significant difference (**$p<0.05$) was registered between native and PGG treated (PGG) samples in circumferential direction; (C) Compliance (max. Force/ Stretch ratio) for native, glutaraldehyde (Glut), decellularized (decell), and PGG treated (PGG.) BJV, calculated from parameters recorded during suture retention testing, N=6, (D) Maximum stress during biaxial testing of native, glutaraldehyde treated fresh (Glut), decellularized (decell), and PGG-treated decellularized (PGG) BJV walls, no significant difference between different orientation of the same sample or same orientation of different samples, N=8; (E) Young's modulus of native, glutaraldehyde treated fresh (Glut),

decellularized (decell), and PGG treated decellularized (PGG) BJV walls, no statistically significant difference between the individual samples, N=8; Stress-strain curves of (F) native, (G) glutaraldehyde treated fresh (Glut), (H) decellularized (decell), and (I) PGG treated decellularized (PGG) BJV, plotted from parameters registered during biaxial testing.

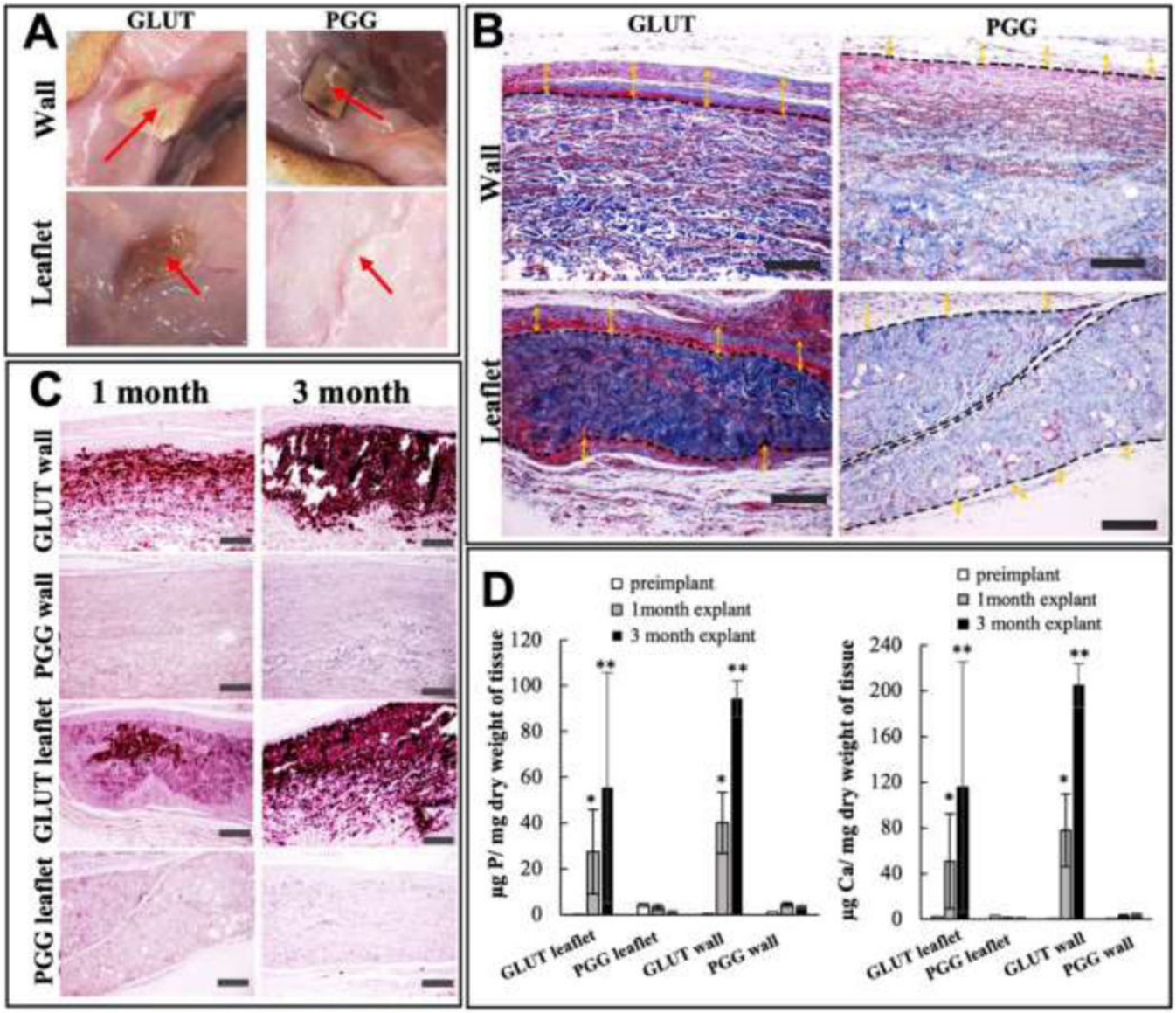

Figure 4:

Biocompatibility assay of glutaraldehyde treated native (Glut) and PGG treated decellularized (PGG) BJV walls and leaflets: (**A**) Gross view of the implants at 30 days post implantation, red arrow: implant at the inner surface of the skin (**B**) Masson's staining of explanted leaflet and wall segments after 30 days of implantation showing thick capsule formation (yellow arrow) around Glut implants with dense cellular infiltration in the capsular area. PGG implants show a loose, capsular area with minimal cell invasion around the implant (scale bar: 200 μm) (**C**) Alizarin red staining showing extensive calcification in Glut walls and leaflets 30 and 90 days after implantation, no calcification observed in PGG scaffolds (scale bar: 200 μm); (**D**) ICP calcium (right) and phosphorous (left) analysis of explanted Glut and PGG tissues, increased levels of minerals in Glut tissues compared to pre-implant and PGG groups. PGG treated tissues did not show elevated calcium or phosphorous levels post implantation; * Significant difference compared to pre-implant and

PGG treated explants, $p<0.001$; ** Significant difference compared to pre-implant, 30-day explant, and PGG treated explants, $p<0.001$ (N=5).

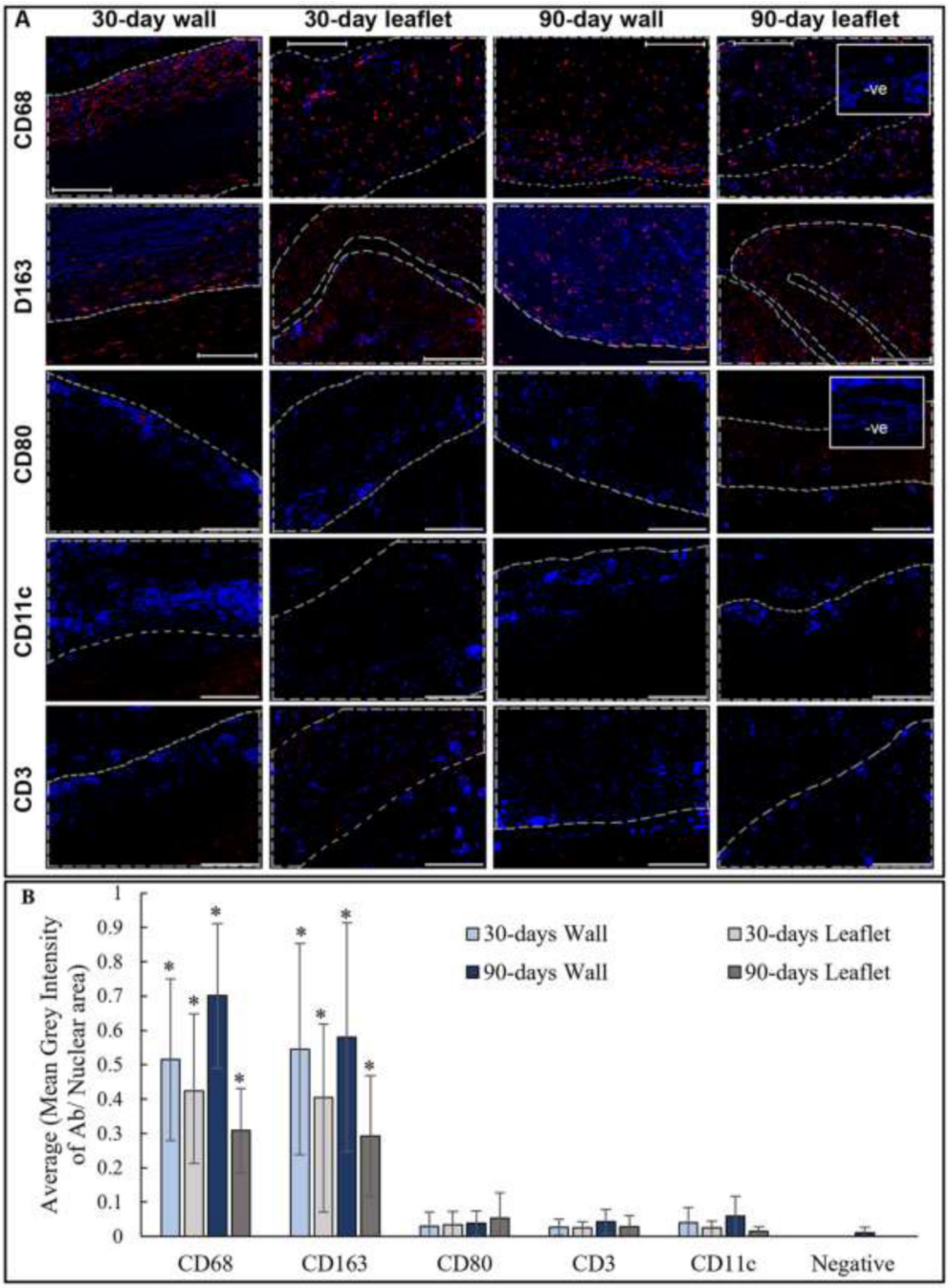

Figure 5:

Immunofluorescence analysis of subcutaneously implanted PGG treated BJV walls and leaflets: (A) Representative images of 30-days and 90-days post implant showing positive staining for CD68 pan-macrophage marker, and CD163 anti-inflammatory (M2) macrophages. No CD80, CD3, or CD11c cells observed (scale bar: 200 μm); Red: positive staining; Blue: DAPI; area within gray line indicates tissue implant; -ve images represent negative controls without primary antibody incubation; (B) Semi-quantification of IHC

images, *p<0.001, significant difference from negative mean grey value/ nuclear expression, N=5.

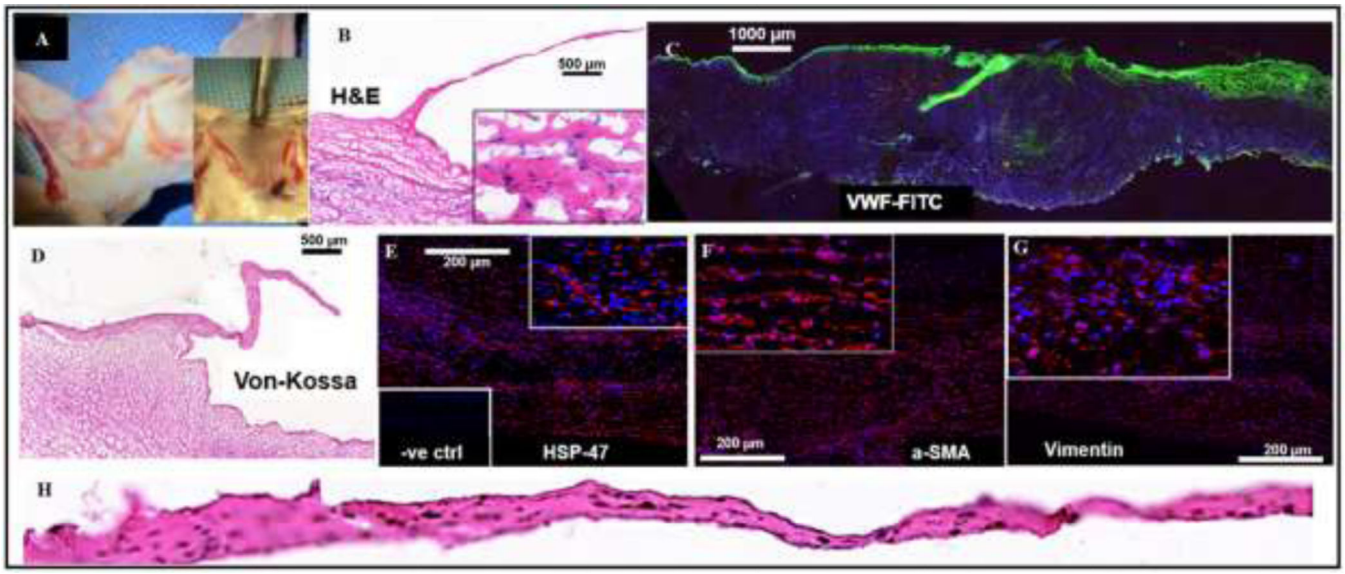

Figure 6:

PGG treated-BJV valved conduits implanted in sheep as pulmonary conduit replacements: (A) Macroscopic view of the explanted leafleted segment of the BJV implant; no tissue overgrowth or thrombosis observed on the walls or leaflets; (B) H&E staining of the implant section, showing cellular infiltration inside the wall region (scale bar: 500 μm); (C) Immunostaining of leaflet section with VWF endothelial marker; leaflets show positive staining, demonstrating luminal reendothelization (scale bar: 1000 μm); (D) Von Kossa staining of BJV section; no calcification present on the wall or leaflet area (scale bar: 500 μm); (E) Immunostaining for HSP-47 antibody, positive staining showing active collagen synthesis in the wall area (scale bar: 200 μm); Immunostaining for α-SMA (scale bar: 200 μm) (F) and Vimentin (scale bar: 200 μm) (G); positive staining showing infiltration of myofibroblast-like cells in the walls; (H) H&E staining of an isolated leaflet, showing cellular infiltration and no thickening.